PALM KERNEL SHELL ASH PARTICLE REINFORCEMENT ON AL-MG-SI AND ITS EFFECT ON THE MECHANICAL AND THERMAL BEHAVIOUR

ABSTRACT

The demand for high-performance materials has increased particularly across all industries in recent times due to the various areas of applications. Industries now require materials with a high strength-to-weight ratio, excellent anti-corrosion properties, good mechanical properties and good thermal conductivity. Given this, this study investigated the effect of palm kernel shell ash particle addition on the mechanical and thermal properties of Al-Mg-Si material. The mechanical properties of aluminium alloy (Al-Mg-Si)/palm kernel shell ash (PKSA) particles composites developed by powder metallurgy method were investigated. Also, Thermo-Gravimetric Analysis (TGA), and Differential Thermal Analysis (DTA) analysis were carried out to determine their thermal properties. The produced PKSA was characterized with XRF to determine its elemental composition and the result showed that the presence of phases such as SiO_2, K_2O and Fe_2O_3 in high proportions which are known to be hard with extreme thermal resistance indicates a better chance at reinforcement. The mechanical properties (hardness, impact strength and flexural deflection) and the thermal properties were used as criteria to access the PKSA reinforced composite. Results revealed that there is an improved mechanical property of the developed composites (with a 47 % increase in the hardness value and 250% increase in the impact strength) which is not farfetched from the reinforcement effect on the reduction in the percentage of elongation.

Keywords: Palm kernel ash; AL-Mg-Si composites; Reinforcements; Microstructure; Mechanical properties

1. INTRODUCTION

The major persuasive reasons for utilizing composites materials particularly over the traditional materials are their high quality, light-weight, improved quality and overall general performance. Composites can be commonly assigned as polymer-matrix composites (PMCs), metal-matrix composites (MMCs) and ceramic-matrix composites (CMCs) based on the variety of matrix material used for development (Sharma et al., 2015; Dawoud and Saleh, 2018). A metal-matrix composite (MMCs) alludes to assembling at least two materials where one matrix phase can be magnesium, aluminium, copper, iron, and so on and the other support phase can be carbides, oxides, nitrides and basic materials,

intentionally added to include the preferred properties. Mostly, the support phase is responsible for the general performance of the created composite. These support face materials could be in form of continuous or discontinuous fibres, whiskers or particles in the matrix to accomplish the blend of better-quality properties. By controlling the addition of the reinforcement in a composite, the preferred properties, for example, strength, stiffness, damping capacity and wear can be additionally upgraded (Rohatgi, 1994; Miracle, 2005). However, the use of naturally sourced agro-waste has been found to be suitable for reinforcement particulate, due to its availability and ease of assessability. Fly ash, red mud, palm oil clinker, rice husk ash, coconut shell debris and sugarcane bagasse are the various sorts of mechanical agro-waste materials used in material reinforcing for the advancement of composites. Immense potentials are required to empower the use of composite materials in different sectors making them fit as aerospace, automotive, construction materials and other engineering applications (Ramachandra and Radhakrishna, 2005; Safiuddin et al., 2010; Alidokht et al., 2011; Lancaster et al., 2013). The use of these wastes as fortifying materials can diminish the natural contamination and the space required for their initial disposal. A thorough literature review on metal-matrix composites using mechanical agro-waste as fortifying materials exists in terms of monolithic composites (single reinforcement) and hybrid composites (more than one fortification materials) (Jayeola et al., 2018; Patil et al., 2018; Venkatesh et al., 2019; Dang, 2019; Mahanta et al., 2019).

2. MATERIALS AND METHODS

2.1 Material

Palm Kernel Shell Ash (PKSA) Preparation

Fresh palm kernel shells (PKS) were obtained from a palm oil processing firm in Ikire, Osun State, South-West, Nigeria. The sample used was a mixture of palm kernel shells from Dura and Pisifera species since the varieties are not habitually sorted during palm oil processing. Before the commencement of the experiment, the shell was sun-dried in an open space at about 32 ^{o}C. The palm kernel shell was crushed with beater crushers that enable the production of small particles. This was further ground in the Pascal L9FS two-roll mill to aid the production of the particle size after which the fresh palm kernel shell was heated in a furnace to a temperature of about 850 ^{0}C. At this stage, the material turned into its carbon ash state which is a popularly known carbonization technique called ‘ashing’.

Al-Mg-Si/PKSA Composites Production

Aluminium alloy (Al-Mg-Si) matrix composites used for this study was obtained by powder metallurgy method carried out in Metallurgical and Materials Engineering Laboratory, Ahmadu Bello University, Zaria, Nigeria. The PKSA compositions of 0, 2, 4, 6, 8, 10, 12, 14, 16, 18, 20 wt% on Al-Mg-Si powder was formulated which correlates to samples C1, C2, C3, C4, C5, C6, C7, C8, C9, C10, C11. The mixed samples were kept in the milling Machine, Pascal L9FS and ball milled with the aid of two roll mills. The operation was done by utilizing rotational cylindrical drum rollers operating in opposing pairs against a flat plate which crushed the materials. The milling was done slowly initially and regulated at a constant speed for about 60 hours, to enable the material to mix homogeneously. The samples were kept under loading for about 5 minutes before they were removed from the mould in preparation for sintering. Furthermore, the samples were compacted to the desired shape and some allowance was given to account for any shrinkage that might occur during the sintering process. The samples were heated to 560 ^{o}C in the furnace which is a temperature that is lower than the melting point of the powdered sample. Thereafter, the samples were left to cool in a controlled atmosphere.

2.2 Mechanical Properties Determination

Micro Hardness

The micro hardness test was conducted using the Rockwell hardness method. Each test samples which were formed to a size of 6.4 mm in size were used per the ASTM E18-79 standard. The indenter (diamond cone or hardened steel ball) of 1.56 mm in size was forced into the test sample with a load of 98.067 N (10 kgf). When equilibrium was reached the indicator device responded to the change in depth of penetration, this was followed by setting the indenter to a datum position. Thereafter, the value was taken directly from the semi-automatic digital scale and recorded.

Impact Strength Determination

The samples were prepared according to the ISO 8256 (2004) standard for DENT as specified (Grellmann, 2007). The dimensions used to determine the impact strength was width of 10 mm, length of 80 mm and height of 64 mm. Notching was carried out with metal blades by a pneumatic notching tool on the thin sides of the sample up to an early crack length of 2 mm, which implies 1 mm on each side. The test was carried out under standard conditions according to ISO 291 (2008) at a temperature of 23 °C and relative air humidity of 50 % as specified (Grellmann, 2007). The samples were fixed parallel between the stationary clamp and the crosshead, the pendulum hammer was set to hit the crosshead at the lowest point of the circular motion. Initially, at the gauge length of 30 mm, the notches were kept in the middle. This corresponded to the hammer speed between 2.9 and 3.7 m/s, then the hammer speed was set in

between 1.0 m/s and 1.5 m/s which corresponded to the falling angle of 40° or 60°. The recorded values of load were analyzed with the aid of extension diagrams according to the service manual of the pendulum device.

Determination of the Flexural Deflection Measurement

The sample was prepared in a rectangular shape with a length of 60.0 mm, a width of 30.0 mm and thickness of 5.0 mm based on the standard test method (ASTM D7028-07-2015) of the flexural strength test, using the Motorized Automatic Recording Tensometer in Mechanical Engineering Department, Laboratory, Ahmadu Bello University, Zaria. Nigeria. The autographic recording drum of the machine was removed and covered with the special graph sheet paper specified for the drum. The sample was installed on the Tensometer by using the flexural fixture and pins to keep it in place. The autographic recording drum was rotated to a suitable starting point and it was ensured that the perspex indicator was set to zero and it was also ensured that the pricker was on the zero axes of the graph sheet. As the load was applied to the samples the amount of elongation or deflection was transmitted via a rotating spindle continually until failure occurred. When the test was completed, the autographic recording drum was removed from the machine and the graph sheet paper was detached from it. On the graph sheet paper, the deflections were evaluated for analysis.

2.3 Thermo-Gravimetric Analysis (TGA/DTA)

The thermo-gravimetric analysis and differential thermal analysis (TGA/DTA) of the samples were conducted using the PerkinElmer TGA 4000 in the Mechanical Engineering Department, Laboratory, Federal University of Technology, Minna. Nigeria. The TGA measures the change in weight of the sample in relation to change in the controlled temperature and these curves showed the thermal scan between 30 °C and 950 °C at 10.00 °C/min during combustion. DTA and Thermo Gravimetric Analysis (TGA) were carried out on the control sample, developed composites and carbonized palm kernel shell at a heating rate of 10 °C/min in a nitrogen atmosphere.

3. RESULTS AND DISCUSSION

The chemical analysis of the palm kernel shell ash (PKSA) was carried out using an X-ray fluorescence (XRF) machine. Result obtained is given in Table 1.

Table 1: Composition of PKSA (wt.%) using XRF

Al_2O_3	SiO_2	P_2O_5	SO_3	K_2O	CaO	TiO_2	Cr_2O_3	MnO	Fe_2O_3	NiO	CuO	Yb_2O_3
7.40	25.30	2.10	1.30	14.90	11.80	0.95	0.28	0.77	12.3	0.20	1.40	0.89

From Table 1, it is observed that major peaks of the chemical composition of the PKS ash were 25.3 wt% Silicon Oxide (SiO_2), 14.9 wt% Potassium Oxide (K_2O), 12.3 wt% Iron Oxide (Fe_2O_3), 11.8 wt% Calcium Oxide (CaO), 7.40 wt%, Aluminum oxide (Al_2O_3) and 2.1 wt% Phosphorus pentoxide (P_20_5) with very notable elements in small proportions. The presence of these elements such as SiO_2, K_2O and Fe_2O_3 in high proportion indicates a better chance as reinforcement (Oyedeji et al., 2021).

3.1 Influence of the Reinforcement on the Mechanical Properties

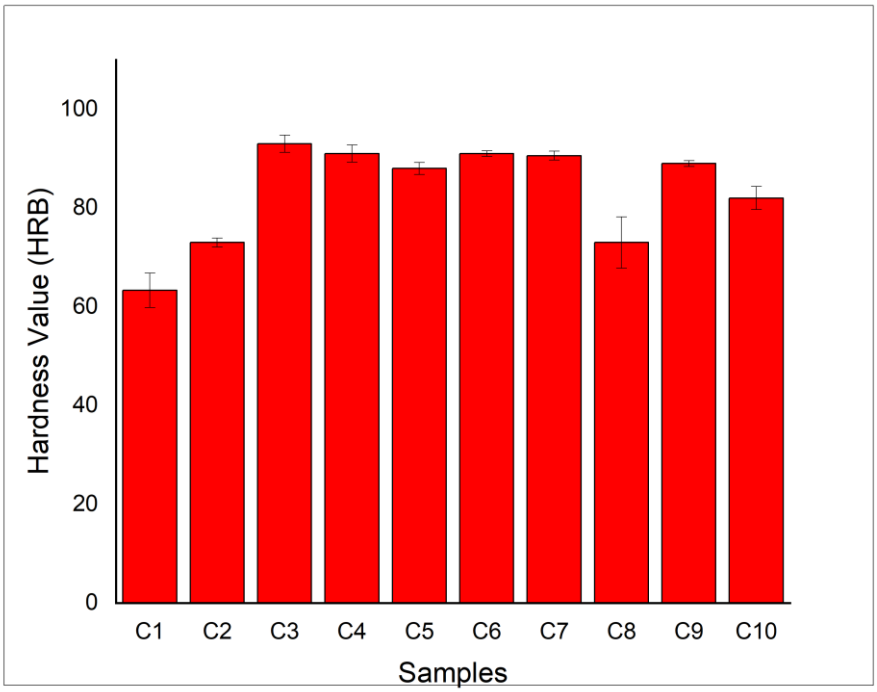

Figure 1: Variation of hardness due to the effect of PKSA particulates addition

As observed in Figure 1, sample C3 which corresponds to 6 wt% PKSA, 94 wt% Al-Mg-Si recorded the highest hardness value of 93 HRB which indicates a 47 % increase in the hardness value of the base sample with no PKSA percentage weight reinforcement (63.3 HRB) as denoted by C1. Similarly, samples C4 and C5 which corresponds to 8 wt% PKSA, 92 wt% Al-Mg-Si and 10 wt% PKSA, 90 wt% Al-Mg-Si both experienced an increase in hardness value due to the effect of PKSA to the matrix. With this occurrence, it is evident that the addition of the reinforcement to powdered alloy showed excellent improvement in the hardness value.

Equally, it can be inferred from this result that the processed PKSA reinforced Al-matrix phase was better than the based sample and this can be attributed to a greater force of adhesion between the processed PKSA and the Al-matrix phase. Similarly, a previous study shows that the addition of frit particles into the Al6061 alloy matrix enhances the hardness of the composites (Ramesh, Swamy, & Chandrashekar, 2010). Though the addition of frit particles at various proportions was from 0 to 10 wt% but in this study, the proportions were up to 20 wt%. It was however noticed that at 20 wt% PKSA addition, the hardness value of the sample which is denoted by C11 was not obtained due to the

drastic drop in the hardness of the sample at this point. This can be attributed to the decrease in the interaction of the particles with each other leading to clustering of particles.

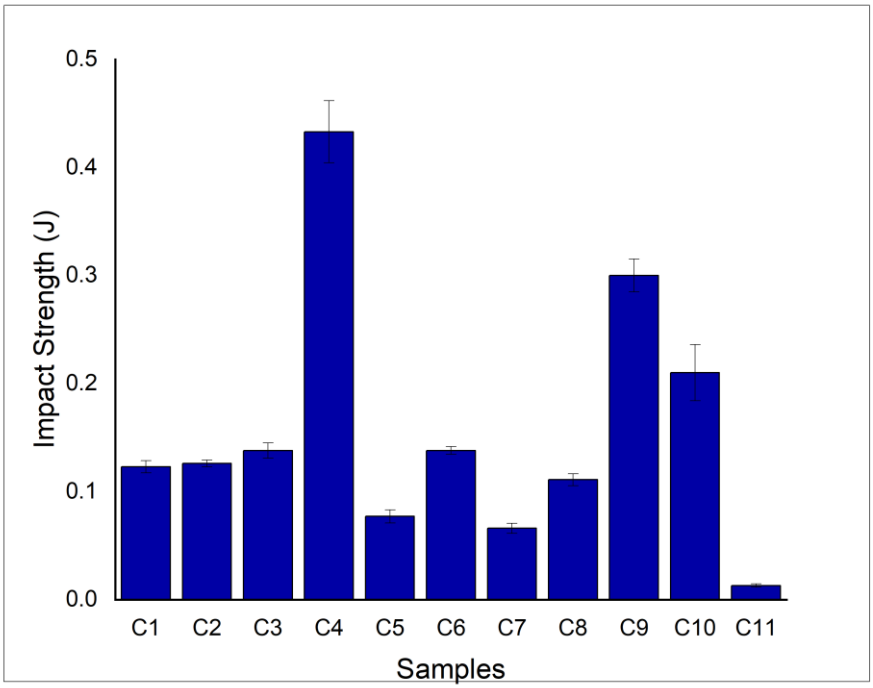

Figure 2: Variation of impact strength due to the addition of PKSA particulates

Result obtained from the impact strength of the samples (Figure 2) showed that sample C4 which consists of 6 wt% PKSA and 94 %wt Al-Mg-Si have the highest impact strength of 0.433 J with a 250% increase in the impact strength as against the base sample. Samples C9 and C10 with 16 wt% PKSA, 84 wt% Al-Mg-Si and 18 wt% PKSA, 82 wt% Al-Mg-Si respectively also had a noticeable increase in impact strength. This could also be a result of the high force of adhesion between palm kernel shell ash and aluminium matrix. Similar to the case of the hardness result, at 20 wt% PKSA addition, the impact strength of the sample which is denoted by C11 reduced drastically. This can be attributed to the decrease in the interaction of the particle with each other leading to the clustering of particles.

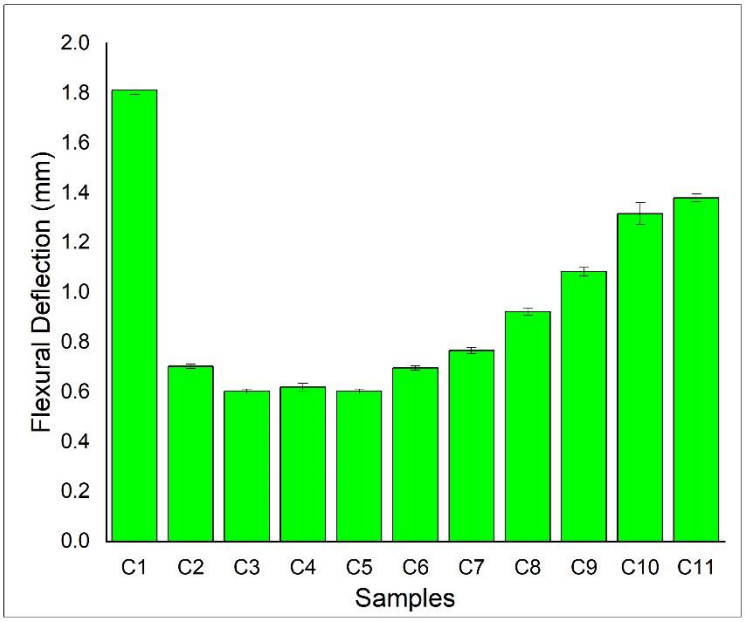

Figure 3: Variation of flexural deflection due to the addition of PKSA particulates

Figure 3 shows the flexural deflection of the samples (C1 to C11) based on the variation in the PKSA percentage weight reinforcement. The result shows that the highest value of flexural deflection is 1.8 mm for the base sample with no PKSA percentage weight reinforcement. This is followed by sample C11 with 20 wt% PKSA with a flexural deflection of 1.4 mm. However, a drastic decrease could be noticed in the transition from sample C1 to C2 which was averagely maintained up to sample C6. A low value of flexural deflection corresponds to an increase in flexural strength of the material. This implies that the addition of PKSA from 2 wt% to 10 wt% resulted in an increase in material strength in comparison with the unreinforced sample. The reinforcement within the particle distribution of the samples could be the contributing factor. Beyond 10 wt%, a reduction in flexural strength which corresponds to an increase in the flexural deflection was noticed. This might have been caused as a result of grain boundaries, crack formation and difficulty in machining.

3.2 Influence of the PKSA on Thermal Analysis of the Composite

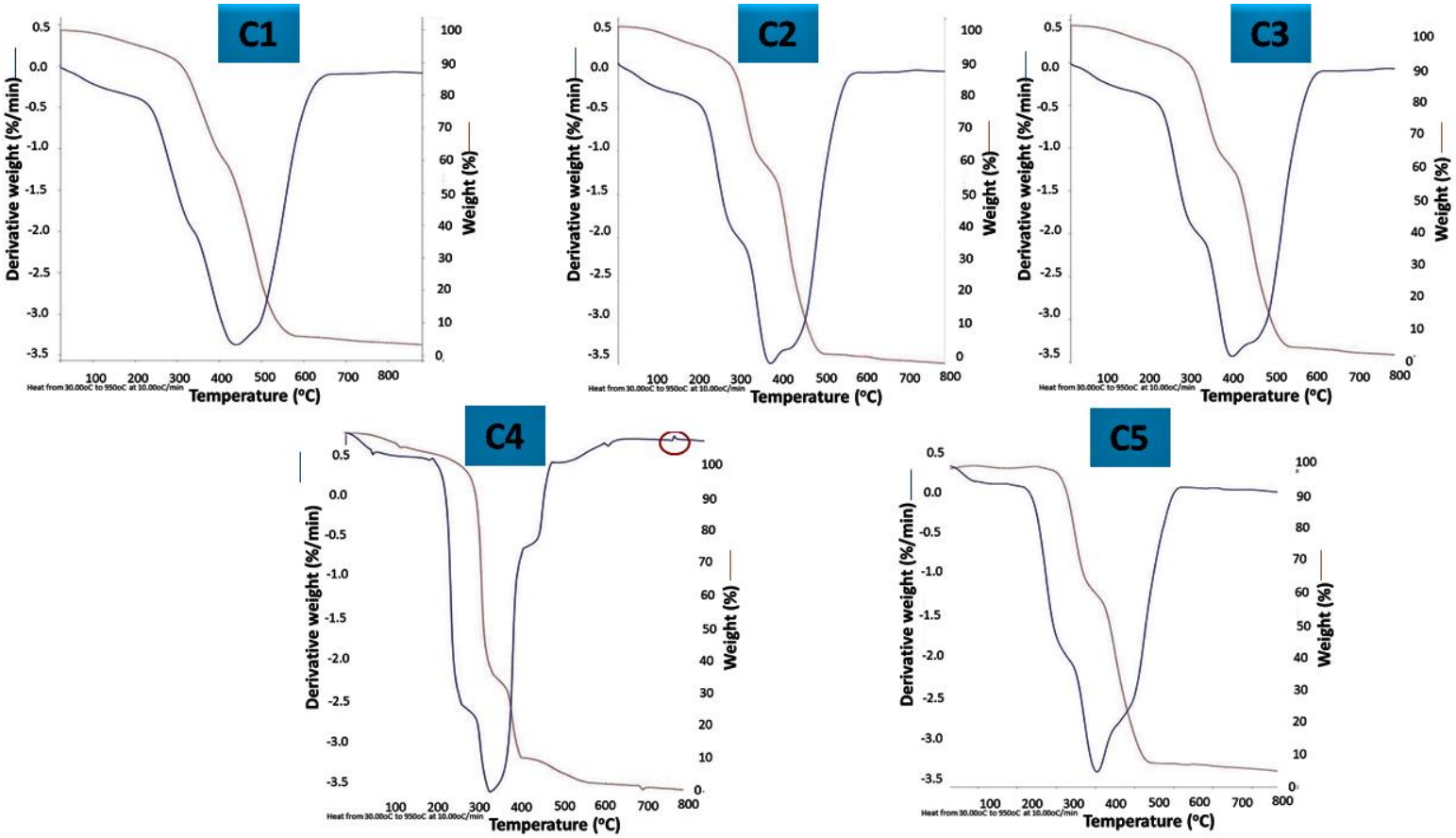

Fig 4: TGA/DTA curves for (6:94) wt.% of PKSA/Al-Mg-Si

From the earlier results obtained from hardness, impact strength and flexural deflection (Section 3.1), thermal analysis was carried out on the control sample (C1) and the samples with promising results (C2, C3, C4, and C5). Figure 4 shows the TGA and DTA curves for these samples which denote compositions of 0, 2, 4, 6, and wt% PKSA/Al-Mg-Si powder. The results show that for all formulations, there was an initial release of moisture at around 150 ^{o}C. This observation is in agreement with the result presented by Wang *et al*., (2009) who observed that the magnitude of the decomposition depends on the material properties and the contact area between the sample and the pan and that the heating rate has a major effect on the results. From the result, the sample with composition (6:94) wt% of PKSA/Al-Mg-Si uniquely peaked at about 770 ^{o}C corresponding to the decomposition of the ingredients in the aluminium melt. The first decomposition was noticed within the range of the onset temperature 300 °C and 370 °C with a corresponding mass depletion of 58 %. The second stage of decomposition was around 370-440 °C with a corresponding mass depletion of 21 % while the third stage of decomposition was found about 440 °C onwards, a plateau region

exhibiting almost constant weight corresponding to about 9 %. The decomposition of samples was a three-step process involving the weight loss in the first stage due to water molecules associated with the crystals corresponding to the drying period. The second step was a rapid loss of mass due to the formation of metal oxide during degradation at which major step in all thermochemical translation process involving biomass occurred and the third stage in which the degression cause a mass loss due to the loss of molecular fragments of the sample or as a result of particles of smoke released from burning caused by inconsistencies in the material itself, beyond the oxidation of carbon.

4. CONCLUSIONS

From this study, the following conclusions are drawn:

i. Palm kernel shell ash (PKSA) particle homogenously mixed in the aluminium alloy matrix and from results, the additions of PKSA particles increased the hardness and considerably decreased the elongation of the composites.

ii. The flexural elongation decreases with increasing constituent composition as well as with the increased ageing time in the heat treatable alloys (Christman et al., 1989).

iii. The strengthening is sustained at high temperatures at a weight fraction of PKSA and decreases hastily when further increased in the composition.

iv. From the result, the sample with composition (6:94) wt.% of PKSA/Al-Mg-Si uniquely peaked at about 770 ^{o}C and another occurred in the range of 600-650 ^{o}C which corresponds to the decomposition of the ingredients in the aluminium melt.

Furthermore, the results show PKSA/Al-Mg-Si based composites have enhanced mechanical properties and can be recommended for use at high temperature, even though doubling the heating rate caused the mass depletion to about 50%. However, the temperature regime for this application area is achieved at the onset temperature of 300 °C.

ACKNOWLEDGEMENT

This study would not have been possible without the support and contributions of other people who sacrificed their time and resources. Words cannot quantify my appreciation to the entire staff of the Department of Mechanical Engineering, and Department of Metallurgical and Materials Engineering, Ahmadu Bello University, Zaria.

CONFLICTS OF INTEREST/COMPETING INTERESTS

The authors declare no conflicts of interest

REFERENCES

Alidokht, S. A., Abdollah-Zadeh, A., Soleymani, S., & Assadi, H. (2011). Microstructure and tribological performance of an aluminium alloy based hybrid composite produced by friction stir processing. *Materials & Design, 32*(5), 2727-2733.

Christman, T., Needleman, A., & Suresh, S. (1989). An experimental and numerical study of deformation in metal-ceramic composites. *Acta Metallurgica, 37*(11), 3029-3050.

Dang, L. C. (2019). *Enhancing the engineering properties of expansive soil using bagasse ash, bagasse fibre and hydrated lime.* UTS Digital Theses Collection.

Dawoud, M. M., & Saleh, H. M. (2018). Introductory Chapter: Background on Composite Materials. *In Characterizations of Some Composite Materials.*

Grellmann, W. S. (2007). *Polymer testing.* Munich: Hanser.

Jayeola, C. O., Adebowale, B. A., Yahaya, L. E., Ogunwolu, S. O., & Olubamiwa, O. (2018). Production of Bioactive Compounds From Waste. *In Therapeutic, Probiotic, and Unconventional Foods*, 317-340.

Lancaster, L., Lung, M. H., & Sujan, D. (2013). Utilization of agro-industrial waste in metal matrix composites: towards sustainability. *In Proceedings of World Academy of Science, Engineering and Technology, 75*, 1136.

Mahanta, S., Chandrasekaran, M., Samanta, S., & Arunachalam, R. (2019). Multi-response ANN modelling and analysis on sliding wear behavior of Al7075/B4C/fly ash hybrid nanocomposites. *Materials Research Express, 6*(8), 085-094.

Miracle, D. B. (2005). Metal matrix composites–from science to technological significance. *Composites science and technology, 65*(15-16), 2526-2540.

Oyedeji, E. O., Dauda, M., Yaro, S. A., & Abdulwahab, M. (2021). The effect of palm kernel shell ash reinforcement on microstructure and mechanical properties of Al-Mg-Si metal-matrix composites. *Proceedings of the Institution of Mechanical Engineers, Part C: Journal of Mechanical Engineering Science*, 09544062211014535.

Patil, P. O., Mahale, S. S., More, M. P., Bhandari, P. V., Deshmukh, P. K., & Bari, S. B. (2018). Eco-Friendly In Situ Fabrication of Reduced Graphene Oxide Gold Nanocomposites for Catalysis and Dye Degradation. *Russian Journal of Physical Chemistry A, 92*(13), 2750-2756.

Ramachandra, M., & Radhakrishna, K. (2005). Synthesis-microstructure-mechanical properties-wear and corrosion behavior of an Al-Si (12%)—Flyash metal matrix composite. *Journal of Materials Science, 40*(22), 5989-5997.

Ramesh, D., Swamy, R. P., & Chandrashekar, T. K. (2010). Effect of weight percentage on mechanical properties of frit particulate reinforced Al6061 composite. *ARPN journal of engineering and applied sciences, 5*(1), 32-36.

Rohatgi, P. K. (1994). Low-cost, fly-ash-containing aluminum-matrix composites. *Jom, 46*(11), 55=59.

Safiuddin, M., Jumaat, M. Z., Salam, M. A., Islam, M. S., & Hashim, R. (2010). Utilization of solid wastes in construction materials. *International journal of physical sciences, 5*(13), 1952-1963.

Sharma, P., Khanduja, D., & Sharma, S. (2015). Production of Hybrid Composite by a Novel Process and its Physical Comparison with Single Reinforced Composites. *Materials Today: Proceedings, 2*(4-5), 2698-2107.

Venkatesh, L., Arjunan, T. V., & Ravikumar, K. (2019). Microstructural characteristics and mechanical behaviour of aluminium hybrid composites reinforced with groundnut shell ash and B 4 C. *Journal of the Brazilian Society of Mechanical Sciences and Engineering, 41*(7), 295.

Wang, S., Tambraparni, M., Qiu, J., Tipton, J., & Dean, D. (2009). Thermal expansion of graphene composites. *Macromolecules, 42*(12), 5251-5255.